Chemistry of Metals and Alloys

Chem. Met. Alloys 3 (2010) 169-176
Ivan Franko National University of Lviv
www.chemetal-journal.org

"Post-hydrogenation" structural transformations from KHg_2- to Fe_2P-type in $R(Cu,Ni)_2$ hydrides (R = Ce, Pr, Nd)

A.B. RIABOV[1]*, R.V. DENYS[1], R. ČERNÝ[2], I.Yu. ZAVALIY[1]

[1] *Physico-Mechanical Institute of National Academy of Sciences of Ukraine, Naukova St. 5, 79601 Lviv, Ukraine*
[2] *Laboratory of Crystallography, University of Geneva, 24 quai Ernest-Ansermet, CH-1211 Geneva 4, Switzerland*
* *Corresponding author. E-mail: alexr@ipm.lviv.ua*

Received June 30, 2010; accepted October 29, 2010; available on-line February 15, 2011

Hydrogenation of orthorhombic KHg_2-type $R(Cu,Ni)_2$ pseudobinary intermetallic compounds (R = Ce, Pr, Nd) was found to lead to the formation of an orthorhombic insertion-type hydride, which readily transforms into a hexagonal Fe_2P-type hydride. This "post-hydrogenation" structural transformation can be accelerated by heating in vacuum at 100-120°C and is accompanied by release of ¼ of the available hydrogen, as has been confirmed by PND studies. Further heating in vacuum leads to disproportionation of the hydride and recombination with recovery of the orthorhombic $R(Cu,Ni)_2$ compound after complete elimination of hydrogen from the material.

Metal hydrides / Crystal structure / X-ray diffraction / Powder neutron diffraction

Introduction

RCu_2 binary intermetallic compounds (IMC), in contrast to Ni- and Co-containing ones with cubic λ_2-$MgCu_2$ type structures, belong either to the AlB_2-type ($LaCu_2$) or the KHg_2-type (also known as $CeCu_2$) – $PrCu_2$ [1]. Our earlier studies were addressed to hydrogenation of La- and Pr-based $R(Cu,Ni)_2$ pseudobinary alloys [2,3]. In both cases the partial substitution of nickel for copper was found to result in stabilization of crystalline hydrides, whereas the $LaCu_2H_{3.3}$ and $PrCu_2H_{\sim 3}$ hydrides were amorphous.

At a lower level of Ni-substitution for Cu ($x \le 0.25$), hydrogenation transforms the structure of $La(Cu_{1-x}Ni_x)_2$ from the AlB_2 to the KHg_2 type. AlB_2-type hydrides are formed by $La(Cu_{1-x}Ni_x)_2$ at $0.4 \le x \le 0.65$ [2]. Freshly prepared hydrides of $Pr(Cu_{1-x}Ni_x)_2$ compounds (x = 0.25, 0.32) retain the symmetry of the initial metal matrix (KHg_2-type). However, after long-term storage the orthorhombic hydrides of $Pr(Cu_{0.75}Ni_{0.25})_2$ and $Pr(Cu_{0.68}Ni_{0.32})_2$ had completely transformed into hexagonal Fe_2P-type hydrides [3].

In contrast to binary hydrides, the formation of which is in most cases accompanied by substantial transformation of the initial metal matrix, in intermetallic hydrides the metal matrix usually preserves the initial symmetry [4]. The examples of substantial change of the symmetry of the metal matrix caused by IMC hydrogenation are rather rare – *e.g.* cubic CsCl-type ZrCo (HfCo) transforms into orthorhombic $ZrCoD_3$ with CrB-type matrix, hydrogenation of orthorhombic YbNi of the FeB type leads to the formation of a cubic hydride (CsCl-type matrix), and HoNiSn (TiNiSi-type) upon hydrogenation becomes hexagonal (ZrNiAl-type matrix) [4]. The last case is similar to the transformation observed in $Pr(Cu,Ni)_2$ compounds because of the structure relations between the TiNiSi and AlB_2 types and between the ZrNiAl and Fe_2P ones. But the structural changes in $Pr(Cu,Ni)_2$, in contrast to the structural changes occurring upon hydrogenation in HoNiSn, were observed in the "post-hydrogenation" period. The proposed reason for such a transformation is the instability of the freshly prepared hydride. However, it was not clear whether such a transition is accompanied by partial release of hydrogen from the hydride or not.

The aim of this paper is to study hydrogenation properties of KHg_2-type compounds of two other light rare earth elements – cerium and neodymium, as well as to determine by neutron diffraction the structures of the orthorhombic and hexagonal hydrides of the $PrCu_{0.75}Ni_{0.25}$ compound within the so-called post-hydrogenation structural transformations.

Experimental part

The alloys for the investigation were prepared by arc-melting of appropriate mixtures of high-grade (> 99.9%) metals in purified argon on a water-cooled copper pad. Rare-earth metals were taken with 1 at.% excess in order to compensate for their partial evaporation during melting. The samples were

homogenized by repeated melting and subsequent vacuum annealing at 600°C for 3 weeks. All parent alloys and corresponding hydrides were characterised by powder X-ray diffraction (Bruker D8, Cu $K\alpha_1$; DRON-3.0, Cu $K\alpha$); their crystallographic parameters were refined using the FULLPROF program [5].

The hydrides were synthesized by hydrogen gas charging of previously activated (heated up to 400°C in vacuum) samples at room temperature. The hydrogenation capacity of the hydrides was monitored by pressure changes in a Sieverts-type apparatus.

For the neutron diffraction analysis deuterium gas (98 % purity) was used instead of hydrogen. Half of the freshly prepared single-phase $Pr(Cu,Ni)_2D_{4.3}$ saturated deuteride was annealed in vacuum at 100 °C for 12 hours in order to accelerate the formation of the lower deuteride. Neutron diffraction data were collected with the HRPT diffractometer at SINQ, PSI, Villigen, Switzerland (λ = 1.494 Å; 2θ range 5…163°, $\Delta\theta$ = 0.05°) [6] two weeks after the synthesis of the deuterides.

Results and discussion

Hydrogenation of $Ce(Cu_{1-x}Ni_x)_2$ and $Nd(Cu_{1-x}Ni_x)_2$ alloys

Crystallographic parameters of the studied KHg_2-type intermetallic compounds and their hydrides are provided in Table 1. As can be seen from the table, the solubility limits of Ni in $CeCu_2$ and $NdCu_2$ are at least x = 0.5 and 0.4, respectively.

Hydrogenation of the $CeCu_2$ alloy, similarly to the earlier studied $LaCu_2$ [2] and $PrCu_2$ alloys [3], leads to its complete amorphization. On the other hand, the $NdCu_2H_{\sim4}$ hydride was found to be poorly crystalline. Such a difference is, perhaps, caused by the slower hydrogenation of the $NdCu_2$ compound, which provides enough time to form crystals of the hydride, which is not the case for the La-, Ce- and Pr-based compounds. All the studied Ce- and Nd-based samples containing both copper and nickel formed well crystallized hydrides. It should be noted that overnight heating of the orthorhombic $Ce(Cu_{0.8}Ni_{0.2})_2H_{4.1}$ hydride in vacuum at 100°C resulted in its complete transformation into the hexagonal hydride, which means that such a procedure is suitable for "ageing" of hydrides.

X-ray diffraction studies of $Pr(Cu_{0.75}Ni_{0.25})_2D_{\sim4}$ and $Pr(Cu_{0.75}Ni_{0.25})_2D_{\sim3}$ deuterides

Freshly deuterated $Pr(Cu_{0.75}Ni_{0.25})_2$ contains a single-phase saturated orthorhombic deuteride (Fig. 1). Its capacity is 4.3 D/f.u. according to volumetric measurements. However, after unloading from the autoclave, the sample can lose some deuterium. The material after heating in vacuum at 120°C was found to be a single-phase Fe_2P-type hexagonal deuteride (Fig. 2). Lattice and atomic parameters of the metal matrix of both deuterides are provided in Table 2.

A pronounced anisotropy of most reflections appears in the diffraction patterns of the hexagonal hydrides. It can originate from 00*l* stacking faults, whereas the reflections of the type h-k = 3n do not reveal such broadening. Compare, for example, the profiles of peaks 111 and 300 (h-k = 3n) on one hand, and of 201, 210 and 211, shown in the inset in Fig. 2, on the other. These two sets of reflections were refined separately with different profile parameters. A similar effect has been observed earlier for Fe_2P-type $La(Cu_{0.35}Ni_{0.65})_2H_{4.0-x}$ [2]. The short c-axis of the unit cell of the hexagonal $Pr(Cu_{0.35}Ni_{0.65})_2D_{\sim3}$ deuteride (4.003 Å) clearly indicates that no short H…H distances similar to those in the structurally related deuteride RNiInD$_{1.33}$ (c = 4.56 Å) [7], can be expected in this structure.

The refined structures of the metal matrix of both hydrides (Table 2) were used for the analysis of available interstices, in order to facilitate the search for deuterium positions. The sizes of the interstices were calculated with the use of the rigid ball model with atomic radii from [8]. For jointly occupied positions (Cu and Ni) the radii were assumed to be an interpolation of r_{Cu} and r_{Ni} taking into consideration the occupancies. The results of the analysis for the orthorhombic and hexagonal hydrides are provided in Tables 3 and 4, respectively. All the interstices in orthorhombic $Pr(Cu_{0.75}Ni_{0.25})_2D_{\sim4}$ are large enough to accommodate hydrogen, the most preferable position for insertion of H atoms being Pr_3M_2 trigonal bipyramids (here and further on M stands for a mixture of Cu and Ni). In the structure of hexagonal $Pr(Cu_{0.75}Ni_{0.25})_2D_{\sim3}$ we can expect insertion of H atoms into Pr_3M_2 trigonal bipyramids, Pr_3M_3 octahedra and some of the Pr_2M_2 tetrahedra. Considering the lower limit of H…H distances (2 Å), the following possible schemes of distribution of H atoms in the hydrides can be proposed (atoms per formula unit, alternative options are given in square brackets):

Orthorhombic $Pr(Cu_{0.75}Ni_{0.25})_2D_{\sim4}$:

1 H in 4e_1 + 1 H in 4e_2 + 2 H in 16j_1 [8f] =
4 H/$Pr(Cu_{0.75}Ni_{0.25})_2$.

Hexagonal $Pr(Cu_{0.75}Ni_{0.25})_2D_{\sim3}$:

⅔ H in 2d [4h] + 1 H in 3g + 2 H in 6j_1 [1 H in 3f_2 +
1 H in 6j_2] = 3.67 H/$Pr(Cu_{0.75}Ni_{0.25})_2$.

These schemes, however, can vary in the case of partial filling of the interstices, which lifts blocking of the occupation of their neighbors.

Analyzing the data provided in Table 3 and 4, one can see that the $KHg_2 \rightarrow Fe_2P$ transformation, which is accompanied by a shift of one of the M atoms (⅓ per formula unit) by ~2 Å = ¼ b_{orth} = ½ c_{hex}, results in the disappearance of some interstices, changes of the array of available tetrahedra and creation of new types of interstice (bold in Table 4). Such a shift leads to the decrease of the total amount of interstices from 14/f.u. to 13⅓/f.u.

Table 1 Crystallographic parameters of $R(Cu_{1-x}Ni_x)_2$ compounds and their hydrides.

Hydride	Structure type of metal matrix	Lattice parameters (Å)			V (Å^3)	$\Delta V/V_0$ (%)	ΔV/H
		a	*b*	*c*			
$CeCu_2$	KHg_2	4.433(1)	7.061(1)	7.472(1)	234.0(1)		
$CeCu_2H_{3.3}$	*Amorphous*						
$Ce(Cu_{0.8}Ni_{0.2})_2$	KHg_2	4.3877(6)	7.1124(8)	7.398(1)	230.88(9)		
$Ce(Cu_{0.8}Ni_{0.2})_2H_{4.1}$	KHg_2	4.4511(6)	8.383(1)	7.948(1)	296.56(7)	28.4	4.0
$Ce(Cu_{0.8}Ni_{0.2})_2H_{4.1-x}$ [a]	Fe_2P	7.6435(6)	–	4.0258(3)	203.69(3)	17.6	3.4
$Ce(Cu_{0.6}Ni_{0.4})_2$	KHg_2	4.367(1)	7.133(2)	7.375(2)	229.7(2)		
$Ce(Cu_{0.6}Ni_{0.4})_2H_{4.2}$	KHg_2	4.441(1)	8.249(3)	7.978(2)	292.2(1)	27.2	3.7
$Ce(Cu_{0.5}Ni_{0.5})_2$	KHg_2	4.325(2)	7.107(4)	7.381(3)	228.5(3)		
$Ce(Cu_{0.5}Ni_{0.5})_2H_{3.8}$	KHg_2	4.453(2)	8.283(4)	7.958(3)	293.5(2)	28.4	4.3
$Pr(Cu_{0.75}Ni_{0.25})_2$	KHg_2	4.3409(2)	7.0991(4)	7.3385(2)	226.15(2)		
$Pr(Cu_{0.75}Ni_{0.25})_2D_{3.8}$	KHg_2	4.4317(5)	8.2291(9)	7.9356(7)	289.40(5)	28.0	4.2
$Pr(Cu_{0.75}Ni_{0.25})_2D_{2.8}$ [a]	Fe_2P	7.5880(6)	–	3.9877(3)	198.84(3)	17.2	3.5
$NdCu_2$	KHg_2	4.3795(8)	7.032(1)	7.407(1)	228.12(7)		
$NdCu_2H_4$	KHg_2	4.3043(7)	9.211(2)	7.808(1)	309.57(9)	34.6	5.1
$Nd(Cu_{0.75}Ni_{0.25})_2$	KHg_2	4.3015(8)	7.070(1)	7.313(1)	222.4(2)		
$Nd(Cu_{0.75}Ni_{0.25})_2H_{4.1}$	KHg_2	4.4106(9)	8.172(2)	7.923(2)	285.6(1)	27.5	3.9
$Nd(Cu_{0.6}Ni_{0.4})_2$	KHg_2	4.3010(9)	7.069(1)	7.312(1)	222.31(8)		
$Nd(Cu_{0.6}Ni_{0.4})_2H_{3.9}$ [b]	KHg_2	4.4589(8)	8.058(2)	7.895(1)	283.65(9)	27.6	3.9
$Nd(Cu_{0.6}Ni_{0.4})_2H_{3.9-x}$ [b]	Fe_2P	7.629(2)	–	4.0125(8)	202.27(7)	21.3	

Notes: [a] after heating in vacuum at 100°C for 12 h; [b] mixture of two hydrides.

Table 2 Atomic parameters of the metal matrix in $Pr(Cu_{0.75}Ni_{0.25})_2$-based deuterides.

Deuteride	Atom	Site	*x*	*y*	*z*	B_{iso} (Å^2)
space group	Pr	4*e*	0	¼	0.499(1)	2.18(6)
Imma	*M*	8*h*	0	0.0118(9)	0.1610(3)	4.4(1)
a = 4.4317(5); *b* = 8.2291(9); *c* = 7.9356(7) Å	R_p=2.28%; R_{wp}=3.07%; χ^2=2.67					
space group	Pr	3*g*	0.6146(3)	0	½	0.93(7)
P-62*m*	*M*1	1*b*	⅓	⅔	0	0.8(2)
a = 7.5845(4)	*M*2	2*c*	0	0	½	2.9(3)
c = 3.9861(2) Å	*M*3	3*f*	0.218(1)	0	0	0.8(2)
	R_p = 2.57 %; R_{wp} = 3.36 %; χ^2 = 2.01					

Note: in the refinement of XRD data all *M* positions were considered as $Cu_{0.75}Ni_{0.25}$

Table 3 Interstices in the structure of orthorhombic $Pr(Cu_{0.75}Ni_{0.25})_2D_{\sim4}$ (based on XRD data).

Int.	Site	Surrounding	*x*	*y*	*z*	r_{int} (Å)	Neighbors
i_1	$4e_1$	TB: Pr_3M_2	0	¾	0.828	0.77[e], 0.69[a]	4×i_3, 2×i_5
i_2	$4e_2$	TB: Pr_3M_2	0	¾	0.172	0.78[e], 0.88[a]	4×i_4, 2×i_5
i_3	$8g_1$	T: Pr_2M_2	¼	0.352	¼	0.59	2×i_1, 2×i_6
i_4	$8g_2$	T: Pr_2M_2	¼	0.649	¼	0.60	2×i_2, 2×i_6
i_5	8*h*	T: Pr_2M_2	0	0.847	0.012	0.53	i_1, i_2, 2×i_7
i_6	$16j_1$	T: Pr_2M_2	0.106	0.500	0.376	0.50	i_3, i_4, i_6, i_7
i_7	8*f*	T: Pr_2M_2	0.733	0	0	0.47	2×i_6, 2×i_5

Note: types of interstice: T – tetrahedron, TB – trigonal bipyramid; [e] – equatorial; [a] – axial radii.

Neutron diffraction study of the $Pr(Cu_{0.75}Ni_{0.25})_2D_{3.5}$ and $Pr(Cu_{0.75}Ni_{0.25})_2D_{2.8}$ deuterides

Neutron diffraction of the sample with single-phase orthorhombic hydride revealed that, two weeks after the preparation, half of the material had transformed into the hexagonal deuteride. We used the following strategy for PND data processing: first, the structure of the hexagonal hydride was determined from the single-phase sample data, and then these results were introduced into the refinements of the two-phase

Table 4 Interstices in the structure of hexagonal $Pr(Cu_{0.75}Ni_{0.25})_2D_{\sim 3}$.

Int.	Site	Surrounding	*x*	*y*	*z*	r_{int} (Å)	Neighbors
i_1	2*d*	TB: Pr_3M_2	⅓	⅔	½	0.53[e], 0.72[a]	6×i_3
Trigonal bipyramid 2*d* can be considered as two tetrahedra 4*h*							
i_1'	4*h*	T: Pr_3M	⅓	⅔	0.453	0.54	
***i*₂**	**3*g***	**O: Pr_3M_3**	**0.227**	**0**	**½**	**spacious**	**2×*i*₂, 2×*i*₃**
i_3	12*l*	T: Pr_2M_2	0.850	0.299	0.226	0.51	i_1, i_5, i_7, i_8
***i*₄**	**6*i***	**T: PrM_3**	**0.856**	**0**	**0.192**	**0.37**	***i*₄, 2×*i*₅, *i*₆**
***i*₅**	**2*e***	**T: M_4**	**0**	**0**	**0.070**	**0.45**	**2×*i*₃, *i*₄**
i_6	3f_2	T: Pr_2M_2	0.763	0	0	0.46	2×i_3, 2×i_7
i_7	6j_1	T: Pr_2M_2	0.251	0.409	0	0.46	2×i_2, i_6, i_8
i_8	6j_2	T: Pr_2M_2	0.062	0.482	0	0.55	2×i_2, i_7, i_8

Note: types of interstice: T – tetrahedron, TB – trigonal bipyramid, O – octahedron; [e] – equatorial; [a] axial radii. New types of interstice formed after transformation are shown in bold.

Table 5 Crystal structure of two-phase $Pr(Cu_{0.75}Ni_{0.25})_2D_{3.5}$ deuteride (R_p = 2.55 %; R_{wp} = 3.40 %; χ^2 = 12.5).

Atom	Site	*x*	*y*	*z*	B_{iso} (Å^2)	Occ.	Occupied polyhedra	r_{int} (Å)
$Pr(Cu_{0.75}Ni_{0.25})_2D_{3.84(8)}$: space group *Imma*; *a* = 4.402(2) Å; *b* = 8.213(3) Å; *c* = 7.951(3) Å; 49(2)%								
Pr	4*e*	0	¼	0.486(4)	2.6(4)	1.0(–)		
¾Cu+¼Ni	8*h*	0	0.009(1)	0.166(1)	4.3(3)	1.0(–)		
D1	8*h*	0	0.197(1)	0.163(2)	2.0(–)	0.5(–)	T: Pr_3M	0.69
D2	8*h*	0	0.681(2)	0.181(3)	2.0(–)	0.36(2)	T: Pr_3M	0.85
D3	16*j*	0.047(4)	0.028(2)	0.640(1)	2.0(–)	0.38(1)	T: Pr_2M_2	0.49
D4	8*h*	0	0.142(2)	-0.010(5)	2.0(–)	0.30(1)	T: Pr_2M_2	0.53
$Pr(Cu_{0.75}Ni_{0.25})_2D_{3.15(8)}$: space group *P*-62*m*; *a* = 7.598(2) Å; *c* = 4.003(1) Å; 51(2)%								
Pr	3*g*	0.612(3)	0	½	0.16(–)	1.0(–)		
0.9Cu1+0.1Ni1	2*c*	⅓	⅔	0	0.62(–)	1.0(–)		
Ni2	1*b*	0	0	½	1.1(–)	1.0(–)		
0.9Cu3+0.1Ni3	3*f*	0.234(1)	0	0	1.20(–)	1.0(–)		
D1	2*d*	⅓	⅔	½	5.7(–)	1.0(–)	TB: Pr_3M_2	0.52[e], 0.73[a]
D2	3*g*	0.218(2)	0	½	0.5(–)	0.74(3)	O: Pr_3CuM_2	*n/a**
D3	6*j*	0.197(3)	0.771(3)	0	3.5(–)	0.87(3)	T: Pr_2M_2	0.45

Note: * Distances from D2 atoms to neighbors: $d_{D2...Ni}$ = 1.656; $d_{D2...M}$ = 2.005; $d_{D2...Pr}$ = 2.560; $d_{D2...Ni}$ = 2.994 Å.

Table 6 Crystal structure of the hexagonal $Pr(Cu_{0.75}Ni_{0.25})_2D_{2.8}$ deuteride (R_p = 2.42 %; R_{wp} = 3.17 %; χ^2 = 8.61).

Atom	Wyckoff site	*x*	*y*	*z*	B_{iso} (Å^2)	Occ.	Occupied polyhedra	r_{int} (Å)
$Pr(Cu_{0.75}Ni_{0.25})_2D_{2.82(3)}$: space group *P*-62*m*; *a* = 7.5815(6) Å; *c* = 3.9840(4) Å								
Pr1	3*g*	0.6138(8)	0	½	0.16(7)	1.0(–)		
0.9Cu1+0.1Ni1	2*c*	⅓	⅔	0	0.62(8)	1.0(–)		
Ni	1*b*	0	0	½	1.1(1)	1.0(–)		
0.9Cu3+0.1Ni3	3*f*	0.2278(4)	0	0	1.20(8)	1.0(–)		
D1	2*d*	⅓	⅔	½	5.7(2)	1.0(–)	TB: Pr_3M_2	0.52[e], 0.72[a]
D2	3*g*	0.2140(7)	0	½	0.5(1)	0.65(1)	O: Pr_3NiM_2	n/a*
D3	6*j*	0.1960(9)	0.7631(9)	0	3.5(1)	0.75(1)	T: Pr_2M_2	0.45

Note: * Distances from D2 atoms to neighbors: $d_{D2...Ni}$ = 1.622; $d_{D2...M}$ = 1.995; $d_{D2...Pr}$ = 2.541; $d_{D2...Ni}$ = 3.013 Å.

sample, and the structure of the orthorhombic deuteride was refined. Then the final refinement of the hexagonal deuteride in the two-phase sample was performed. Results of the structure refinement are provided in Tables 5 and 6, the corresponding PND patterns are shown in Figs. 3 and 4, and the structures of both types of hydride are shown in Fig. 5.

As can be seen from the results of the refinement, the D1 and D2 atoms in the structure of orthorhombic $Pr(Cu_{0.75}Ni_{0.25})_2D_{3.8}$ are shifted from the centers of the

Table 7 Distribution of D atoms in the structures of $Pr(Cu_{0.75}Ni_{0.25})_2$-based deuterides (in D/f.u.).

Orthorhombic deuteride		Hexagonal deuterides		
	$Pr(Cu_{0.75}Ni_{0.25})_2D_{3.84}$		$Pr(Cu_{0.75}Ni_{0.25})_2D_{3.15}$	$Pr(Cu_{0.75}Ni_{0.25})_2D_{2.82}$
D1	1(–)	D1	0.67(–)	0.67(–)
D2	0.72(4)	D2	0.74(3)	0.65(1)
D3	1.52(4)	D3	1.74(6)	1.50(2)
D4	0.60(2)			

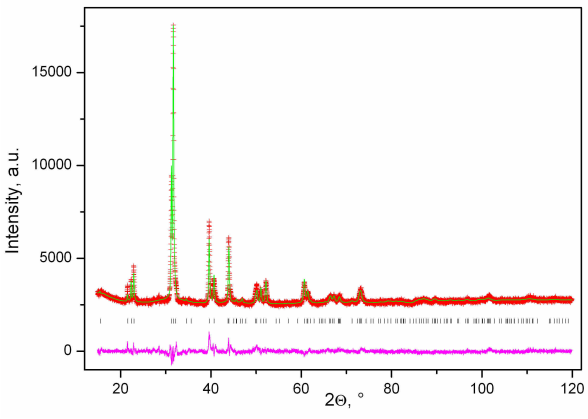

Fig. 1 Observed (+), calculated (upper line) and difference (lower line) X-ray diffraction pattern of freshly prepared single-phase $Pr(Cu_{0.75}Ni_{0.25})_2D_{\sim 4}$. Positions of the Bragg reflections are shown as vertical bars.

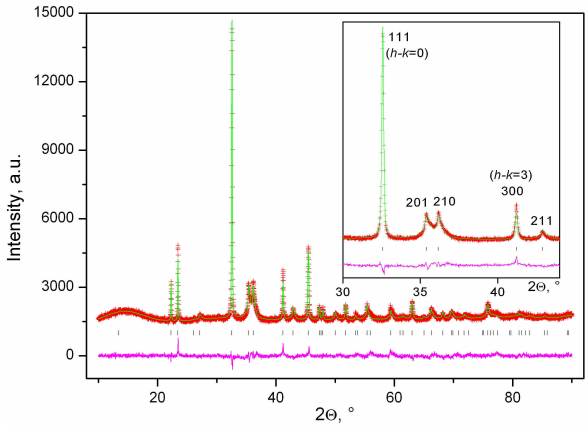

Fig. 2 Observed (+), calculated (upper line) and difference (lower line) X-ray diffraction pattern of single-phase hexagonal $Pr(Cu_{0.75}Ni_{0.25})_2D_{\sim 3}$. The difference in profile parameters of h-k = 3n reflections and others is illustrated in the inset.

trigonal bipyramids, occupying their tetrahedral halves (see Fig. 5*a*), which means that the occupancy of those positions cannot exceed 50 % because of too short D...D distances ($\delta_{D1...D1}$ = 0.88 Å, $\delta_{D2...D2}$ = 1.12 Å). In addition, the D3 atoms have 50 % as higher occupancy limit as well ($\delta_{D3...D3}$ = 0.41 Å). The refined D1...D3 positions agree well with the proposed model of the structure. However, the shift of the D2 position from the centre of the Pr_3M_2 trigonal bipyramid into one of its halves allows additional partial filling of the D4 site, not foreseen in the model.

In the structures of the hexagonal $Pr(Cu_{0.75}Ni_{0.25})_2D_{3.15}$ (in the two-phase $Pr(Cu_{0.75}Ni_{0.25})_2D_{3.5}$ sample) and $Pr(Cu_{0.75}Ni_{0.25})_2D_{2.82}$

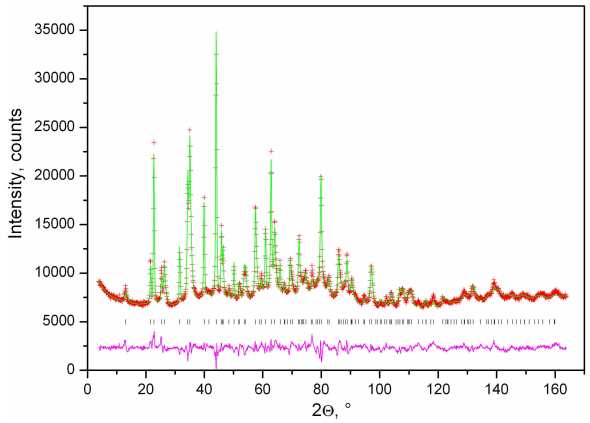

Fig. 3 Observed (+), calculated (upper line) and difference (lower line) PND patterns of hexagonal $Pr(Cu_{0.75}Ni_{0.25})_2D_{2.82}$ deuteride.

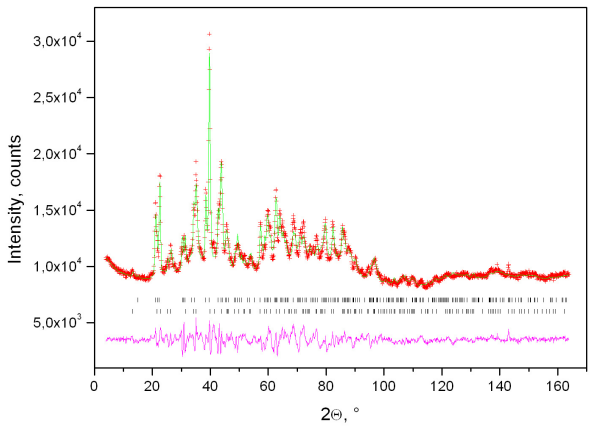

Fig. 4 Observed (+), calculated (upper line) and difference (lower line) PND patterns of a mixture of orthorhombic $Pr(Cu_{0.75}Ni_{0.25})_2D_{3.84}$ (upper set of Bragg peak positions) and hexagonal $Pr(Cu_{0.75}Ni_{0.25})_2D_{3.15}$ deuterides.

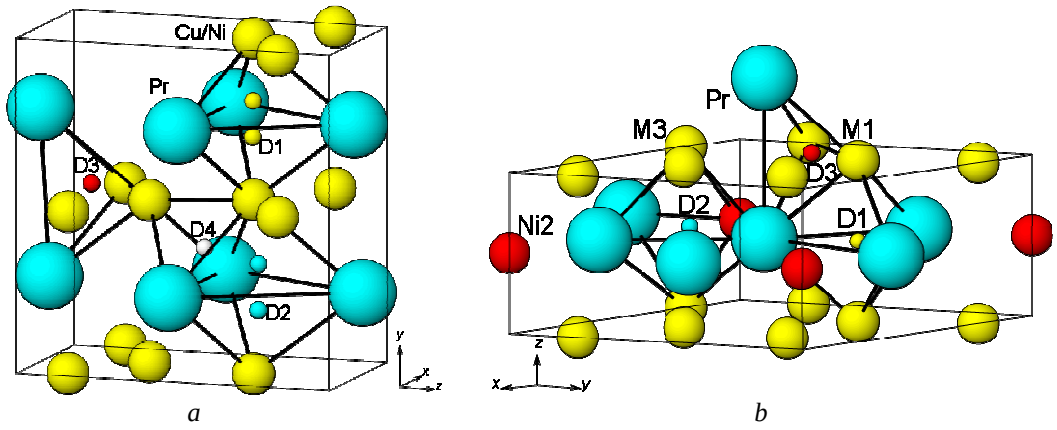

a *b*

Fig. 5 Crystal structures of the orthorhombic $Pr(Cu_{0.75}Ni_{0.25})_2D_{3.84}$ (*a*) and hexagonal $Pr(Cu_{0.75}Ni_{0.25})_2D_{2.82}$ (*b*) deuterides.

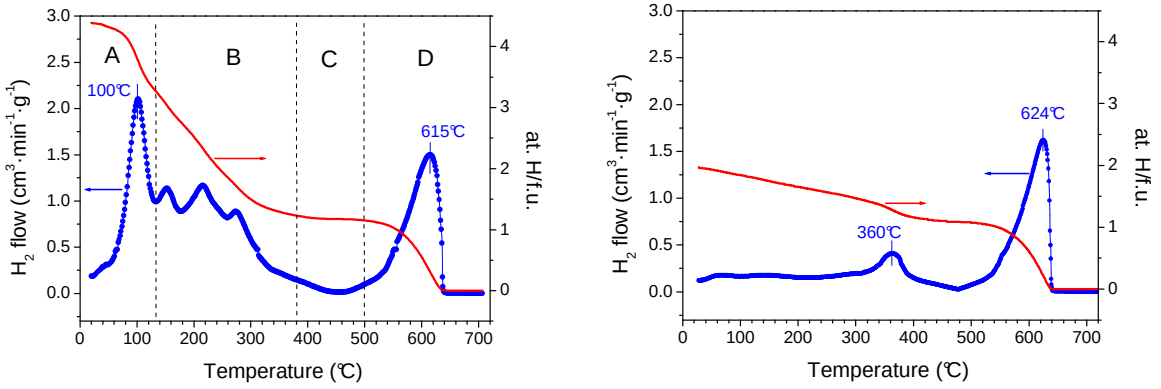

a *b*

Fig. 6 Hydrogen thermal desorption traces in vacuum for freshly prepared $Pr(Cu_{0.75}Ni_{0.25})_2H_{4.3}$ hydride (*a*) and the same material after disproportionation in H_2 at 400°C (*b*) (2°C/min, changes of the hydrogen content are presented on a unified scale).

deuterides three types of interstice are occupied: trigonal bipyramid Pr_3M_2, distorted octahedron Pr_3M_3Ni and tetrahedron Pr_2M_2. The first two occupied sites are similar to those filled in the structures of $RNiAlH_x$ [9] (trigonal bipyramid) and $LaNiInD_{1.63}$ [10] (distorted octahedron). The difference in the hydrogen content in these two hexagonal hydrides is caused by different occupancies of the D2 and D3 sites (74 and 87 % in the hydride during transformation, compared to 65 and 75 % in the "aged" hydride, see Table 7).

The analysis of the available interstices in both types of structure reveals that the radii of all interstices exceed the lower limit of 0.4 Å. Some of the interstices in the orthorhombic hydrides are larger than in the hexagonal ones (compare the sizes of available trigonal bipyramids). The size of the interstices in the orthorhombic hydride can be one of the driving forces of the *ortho-hex* transformation. As can be seen from Table 1, in the orthorhombic hydride the increment of the unit cell volume per absorbed H atom is 4.2 $Å^3$/H, whereas in the hexagonal hydride this value is 3.5 $Å^3$/H. The last value is much closer to the usually observed range of 2...3 $Å^3$/H. One more reason for the decrease of the volume increment is the decrease of the total number of interstices per formula unit from 14 to 13⅓ (compare data in Tables 3 and 4).

Hydrogenation-dehydrogenation peculiarities of $Pr(Cu_{0.75}Ni_{0.25})_2$

In order to clarify the mechanism of the $Pr(Cu,Ni)_2D_x$ *ortho* → $Pr(Cu,Ni)_2D_x$ *hex* transformation we have performed an additional study of the hydrogenation properties of the $Pr(Cu_{0.75}Ni_{0.25})_2$ alloy. The alloy was first hydrogenated under 25 bar H_2 without preliminary activation, reaching the composition $Pr(Cu_{0.75}Ni_{0.25})_2H_{4.3}$ after 2 hours. The prepared hydride was tested by TDS without unloading from the autoclave. No hydrogen release was observed at room temperature after evacuating the

system (10^{-5} mbar). During heating in vacuum, the sample starts desorbing above room temperature. The strong peak in the 50-130 °C range (Fig. 6*a*) corresponds to the loss of ~1 H/f.u. and is apparently associated with the $KHg_2 \rightarrow Fe_2P$ transition. Further heating up to 380°C leads to desorption of two more H/f.u., reaching the $Pr(Cu_{0.75}Ni_{0.25})H_{1.2}$ composition. No hydrogen desorption is observed in the 380…500°C temperature window. After that, a rather strong desorption peak at a temperature of 615°C appears. The last desorption peak can reasonably be attributed to hydrogen desorption from praseodymium dihydride (675°C at 5°/min heating rate [11]). Accounting for this, one can conclude that, after desorption of > 70 % of the hydrogen, the material seems to decompose into a mixture containing PrH_2. The possible scheme of the desorption process is (letters correspond to temperature ranges in Fig. 6*a*):

A. Partial hydrogen desorption (~¼ of the total H content) from KHg_2-type hydride. Structure transformation to Fe_2P-type hydride: PrM_2H_{4+x} *ortho* $\rightarrow PrM_2H_{3+x}$ *hex* + ½ H_2;

B. partial desorption from Fe_2P-type hydride: $PrM_2H_{3+x} \rightarrow PrM_2H_{1.2} + H_2$;

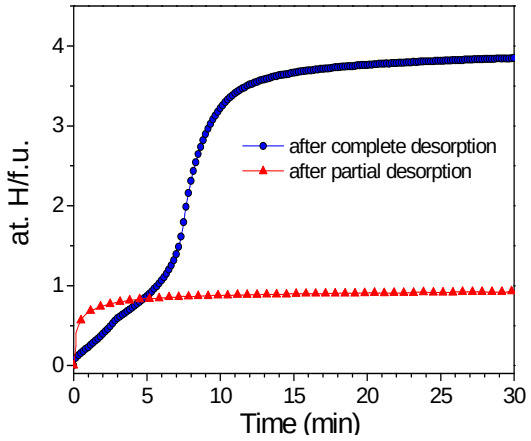

Fig. 7 Repeated hydrogen absorption by $Pr(Cu_{0.75}Ni_{0.25})_2$ after complete recombination during desorption, and after partial hydrogen release up to 120°C.

C. Disproportionation $PrM_2H_{1.2} \rightarrow$ 0.6 PrH_2 + 0.4 PrM_5 (such a reaction is clear from the quantity of hydrogen desorbed above 500°C);

D. Recombination 0.6 PrH_2 + 0.4 $PrM_5 \rightarrow PrM_2$ *ortho* + 0.6 H_2.

The disproportionation of the intermetallic hydride $PrM_2H_{1.2}$ may be caused by its lower thermodynamic stability as compared with binary PrH_2. In addition we carried out the usual procedure of disproportionation by heating the saturated hydride in hydrogen up to 400°C. Hydrogen desorption traces from the disproportionation products are shown in Fig. 6*b*. As can be seen from a comparison of Figs. 6*a* and 6*b*, the hydrogen content in the disproportionated mixture is twice lower than in the saturated hydride. The position and intensity of the peak at ~620°C clearly confirm that it can be attributed to hydrogen desorption from PrH_2 dihydride, which is accompanied by 0.6 PrH_2 + 0.4 $PrM_5 \rightarrow PrM_2$ + 0.6 H_2 recombination. Moreover, the peak at 360°C, not observed in Fig. 6*a*, corresponds to hydrogen desorption from octahedral interstices in PrH_{3-x} hydride [11].

After complete hydrogen desorption, the sample was saturated under 1 bar hydrogen again (Fig. 7); the hydrogenation capacity was found to decrease only slightly. After repeated synthesis, the saturated hydride was heated in vacuum up to 100°C and then cooled down to room temperature. After that it appeared to absorb 1 bar hydrogen in the quantity of 1 H/f.u., forming the orthorhombic hydride, and proving by this that the *ortho-hex* transformation is reversible.

Conclusions

1. In the case of hydrides based on KHg_2-type $R(Cu,Ni)_2$ compounds (R = Ce, Pr, Nd), for some compositions long-time storage or heating up to ~100°C results in a transformation of the orthorhombic hydride (filled KHg_2-type) to a hexagonal one (filled Fe_2P-type).
2. Neutron diffraction studies of orthorhombic and hexagonal $R(Cu_{0.75}Ni_{0.25})_2D_x$ deuterides revealed that the *ortho-hex* transformation is accompanied by release of one quarter of the hydrogen of the saturated sample (the D content decreases from ~4 to ~3 D/f.u.). This leads to a decrease of the unit cell volume increment from 4.2 to 3.5 Å^3 per absorbed hydrogen atom.
3. A hydrogen thermal desorption experiment for $Pr(Cu_{0.75}Ni_{0.25})_2H_{4.3}$ indicated that the *ortho-hex* transformation occurs around 100 °C and is followed by disproportionation and recombination of the material.

References

[1] P. Villars, K. Cenzual, J. Daams, F. Hulliger, T. Massalski, H. Okamoto, K. Osaki, A. Prince (Eds.), *Pauling File, Binaries Edition*, ASM International, Materials Park, OH, 2002.
[2] R.V. Denys, I.Yu. Zavaliy, R. Černý, I.V. Koval'chuck, *J. Alloys Compd.* 396 (2005) 139-142.
[3] I.Yu. Zavaliy, R. Černý, V.N. Verbetsky, R.V. Denys, A.B. Riabov, *J. Alloys Compd.* 358 (2003) 146-151.
[4] V.A. Yartys, A.B. Riabov, M.V. Lototsky, *Materials Science and Crystal Chemistry of Intermetallic Hydrides*, Spolom, Lviv, 2006, 288 p.
[5] J. Rodriguez-Carvajal, *Physica B* 192 (1993) 55.
[6] P. Fischer, G. Frey, M. Koch, M. Könnecke, *Physica B* 276-278 (2000) 146-147.

[7] O. Ardelean, G. Blanita, G. Filoti, P. Palade *J. Phys.: Conf. Series* 182 (2009) 012045.
[8] W.B. Pearson, *The Crystal Chemistry and Physics of Metals and Alloys*, Wiley-Interscience, New York, London, Sydney, Toronto, 1972.
[9] B.C. Hauback, H. Fjellvåg, L. Pålhaugen, V.A. Yartys, K. Yvon, *J. Alloys Compd.* 293-295 (1999) 178-184.
[10] R.V. Denys, A.B. Riabov, V.A. Yartys, B.C. Hauback, H.W. Brinks, *J. Alloys Compd.* 356-357 (2003) 65-68.
[11] V.A. Yartys, O. Gutfleisch, V.V. Panasyuk, I.R. Harris, *J. Alloys Compd.* 253-254 (1997) 128-133.

Proceeding of the XI International Conference on Crystal Chemistry of Intermetallic Compounds, Lviv, May 30 - June 2, 2010.